Shear Systematics in Simulated LSST Images

Chihway Chang[1], Steven M. Kahn[1], J. Garrett Jernigan[2], John R. Peterson[3], Andrew P. Rasmussen[1]
Justin Bankert[3], A. J. Connolly[4], Emily Grace[3], Kirk Gilmore[1], Rob Gibson[4], Lynne Jones[4], Simon Krughoff[4],
Suzanne Lorenz[3], Stuart Marshall[1], Jim Pizagno[4], Nicole Sylvestre[4], Nathan Todd[3], Mallory Young[3]

[1]KIPAC/SLAC, [2]SSL/UCB and KIPAC/SLAC, [3]Purdue Univ., [4]Univ. Of Washington

The Large Synoptic Survey Telescope (LSST) is a large-aperture, wide-field, ground-based telescope designed to provide a complete survey of 20,000 square degrees of sky in six optical bands every few nights. Over ten years of operation, it will measure the magnitudes, colors, and shapes of several billion galaxies. As such, LSST will probe cosmic shear down to levels far beyond those accessible with current surveys. The unprecedented statistical power of LSST will impose new requirements on the control of weak lensing systematics. Various noise sources become important in this context, associated with counting statistics, atmospheric effects, and wavefront errors introduced by the telescope and camera systems.

We study these various noise components and their impact on shear measurements in single LSST exposures using simulated images produced by a prototype high fidelity photon-by-photon Monte Carlo code. The code includes the most significant physical effects associated with photon propagation through the atmosphere, reflection off of the three mirror surfaces of the telescope, and propagation through the elements of the camera and on into the detector. We report on preliminary results from this program, including plots of residual shear error correlation functions for realistic LSST operating conditions.

Motivation

One of the main goals for LSST is to probe the large scale structure of the total matter distribution in the Universe, the “cosmic shear”, using weak gravitational lensing [1]. Previous surveys were limited by statistical errors associated with the intrinsic shapes of galaxies. For limited sky coverage, this is the dominant contributor to the uncertainty. With LSST, we will reduce this contribution by orders of magnitude, suggesting that we may be limited by systematic errors for the first time. It is therefore necessary to study the potential sources of systematics in LSST images [2].

This is a preliminary report on a larger effort to quantitatively account for expected sources of error in shape measurements of galaxies with LSST and their correlations with angular scale. We invoke a high fidelity simulator, which accounts for most known properties of the atmosphere and the telescope/camera system. Here, we present analyses of noise contributions due to the atmosphere and expected optical aberrations for single LSST exposures.

Simulation

The LSST Image Simulator [3] has been developed to support software development for the LSST data management effort, and to provide high fidelity LSST images for the community for evaluation in terms of expected scientific performance.

Unlike most previous image simulation efforts in optical astronomy, a photon-by-photon Monte Carlo approach is adopted to capture subtle features in the images that would otherwise be hard to account for accurately. Photons are generated from a realistic catalog of objects on the sky and then propagated through the atmosphere and optics and on into the detector. Examples of the physical effects correctly implemented in the simulator are:

- Refraction and diffraction by turbulent cells in the atmosphere. We have constructed a realistic atmospheric model with appropriate parameters for the LSST site [4]
- Stochastic perturbations to the mirror and lens surfaces and misalignments within the adopted build tolerances [5]
- Pointing and tracking errors within adopted tolerances
- Charge diffusion in the silicon detector as expected based on lab data of prototype LSST CCDs
- Background variations for a realistic sky model for the LSST site [6]

The conceptual picture of the ray tracing for each individual photon is shown below:

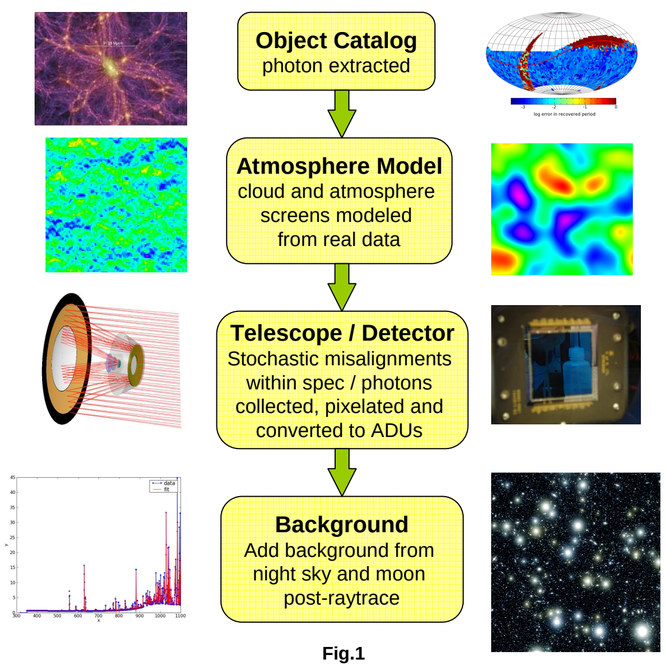

Fig.1

Project Outline

In this study, we generate ensembles of customized images using the simulator in order to understand quantitatively the ultimate uncertainties on shape measurements in a single LSST 15 second exposure. The uncertainty is quantified by σ_{ε_1} and σ_{ε_2}, the standard deviation in the shape parameters, $\varepsilon_1, \varepsilon_2$, over the ensemble of identical input objects. Note that we are primarily interested in stochastic sources of errors that cannot be corrected by continuous monitoring of the system response. Measurable wavefront errors are assumed to be corrected via the active optics control of the mirrors, in accordance with the LSST design, but there are residual wavefront errors that cannot be corrected.

We have not yet accounted for the reduction in noise contributions due to the extensive set of multiple images (~several hundred in each color) that LSST will acquire for all fields. However, understanding noise in a single exposure is a necessary first step to understanding noise in final analyses. We comment at the end about how we expect the errors to scale when multiple images are combined.

Procedure

We systematically study a collection of objects with different sizes and magnitudes; a subset of which is shown in Figure 2. The choice of size range is matched to typical galaxy sizes, while the magnitude range is limited by saturation and detectability under a typical 22 mag/arcsec^2 sky background in a single exposure. Without loss of generality, all extended objects are modeled as r-band circular Gaussians. Four major noise sources are included: counting statistics, optics aberrations, tracking errors and atmospheric distortions. For each run, certain noise sources are turned on and all object are realized 8000 times individually to get a proper statistical sample.

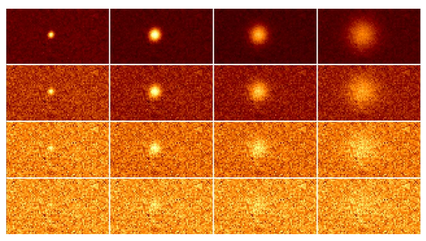

Fig.2 Simulated r-band objects of different size and magnitude. The left column are point sources of magnitude 18, 19, 20, 21(top to bottom). Other three columns are circular Gaussian shapes with input FWHM 1.1”, 2.1” and 3.5” (left to right) scaled to the magnitude that yields roughly the same surface brightness as the star on left.

Shape Measurements

We use the shape parameter “ellipticity” $\varepsilon = (\varepsilon_1, \varepsilon_2)$ as a quantitative measure of the object shapes. A common definition of ellipticity is used:

$$\varepsilon_1 = \frac{\iint I(\vec{\theta})W(\vec{\theta})(\theta_1^2 - \theta_2^2)d\theta_1 d\theta_2}{\iint I(\vec{\theta})W(\vec{\theta})(\theta_1^2 + \theta_2^2)d\theta_1 d\theta_2}, \qquad \varepsilon_2 = \frac{\iint I(\vec{\theta})W(\vec{\theta})(2\theta_1\theta_2)d\theta_1 d\theta_2}{\iint I(\vec{\theta})W(\vec{\theta})(\theta_1^2 + \theta_2^2)d\theta_1 d\theta_2}$$

where $\varepsilon_1, \varepsilon_2$ are estimated from a combination of weighted second moments of the light intensity.

Operationally, software packages Source Extractor [7] and IMCAT [8] were used to detect objects and measure shapes.

Counting Statistics (CS)

Noise due to counting statistics comes from the Poisson nature of the finite numbers of photons. We can quantify the resulting uncertainty in $\varepsilon_1, \varepsilon_2$ as a function of the input size and magnitude. A semi-empirical formula that accurately describes this contribution is:

$$\sigma_{\varepsilon_i} = 1.0338 \times \nu^{-1.0787} + 0.0028 \times r_g^{-1.3754}, i = 1,2$$

where r_g and ν are IMCAT parameters: r_g is the RMS radius in pixels that gives the maximum signal-to-noise ratio ν.

Optics Aberration (OPT)

Residual optics aberrations, outside detectable limits, are modeled in the simulator as Zernike polynomial deformations of the three mirrors and random misalignments of the telescope body. Their effect is generally negligible compared to counting statistics, but becomes important when the object is bright and small (see Figures 4 and 5). A semi-empirical formula that describes the noise due to optics aberrations is:

$$\sigma_{\varepsilon_i} = 1.9393 \times 10^{-3} \times \nu^{0.6621} \times r_g^{-3.5018}, i = 1,2$$

Tracking Error (TR)

The LSST telescope is designed to track within 50 milli-arc seconds per 15 s exposure. The results show that tracking errors have almost no effect on the noise in $\varepsilon_1, \varepsilon_2$ (see Figures 4 and 5).

Atmospheric Distortions (ATM)

The atmosphere variation is complicated. In the simulator, the atmosphere model includes night-to-night and seasonal changes in seeing, wind speed and wind direction. For this study, we constrain the seeing to maintain typical values of approximately 0.7”. The results show the noise on ellipticity measurements due to the atmosphere behaves qualitatively very similarly to that due to optics aberrations; however, the level is higher especially for small, bright objects. A semi-empirical formula that describes the noise due to the atmospheric distortions is:

$$\sigma_{\varepsilon_i} = 0.0112 \times \nu^{0.4459} \times r_g^{-3.3134}, i = 1,2$$

Qualitative behaviors of the four noise components discussed above are visualized in Figure 3.

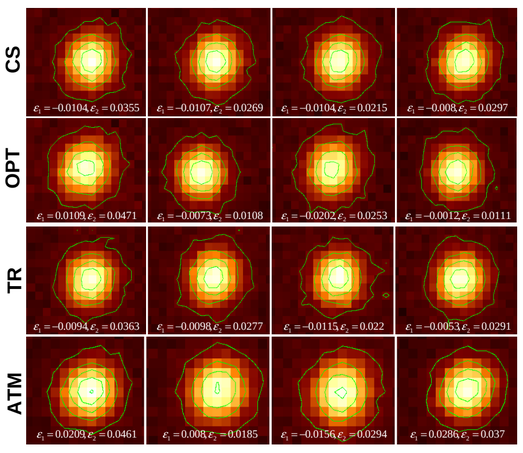

Fig.3 Effects on object shapes due to the four noise sources: counting statistics (CS), optics aberrations (OPT), tracking errors (TR) and atmosphere distortion (ATM). In each row, four out of the ensemble of individual realizations of the same object are shown. The measured ellipticities are listed in the bottom for each object. Note in the last row, objects are selected to have roughly the same seeing to show the effects on shapes only.

[1] The LSST sicence book, version 2.0 [2] Hoekstra and Jain, 2008
[3] The LSST Image Simulation Team website http://lsst.astro.washington.edu/

Results

A summary of the behavior of the four noise components as a function of object size and magnitude is given in Figures 4 and 5 below.

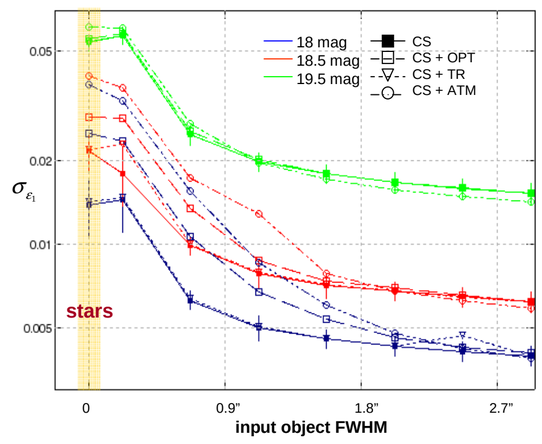

Fig.4 Errors on derived ε_1 (σ_{ε_1}) vs. input object FWHM size plotted for objects of different scaled magnitudes (the magnitude at 500 nm of a star that has roughly the same surface brightness as the object). The plotted magnitude range is chosen to demonstrate differences between the four noise sources. Results for fainter objects are shown in Figure 5. Error bars are plotted for the CS only case.

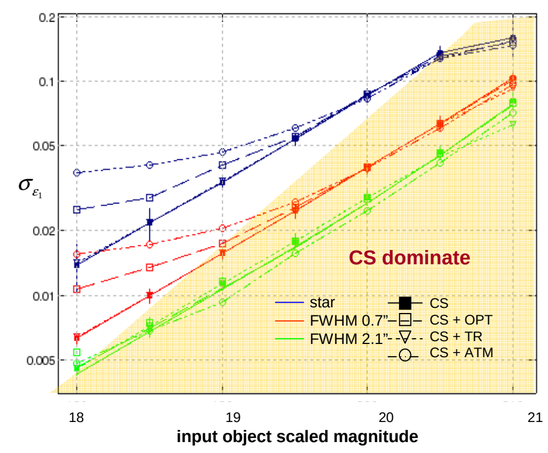

Fig.5 Errors on derived ε_1 (σ_{ε_1}) vs. input object scaled magnitude (defined in Figure 4.) plotted for objects of different input FWHM. Shaded area indicates the region where CS dominate. Error bars are plotted for the CS only case.

From Figure 4 and 5, it is clear that in a single exposure, noise due to photon statistics dominates in most of the cases. Only when the object is bright and small do the other noise components contribute significantly.

Correlations of Noise

For cosmic shear studies, the level of the noise is irrelevant if the errors have no spatial correlation. We calculate the two-point correlation statistics for errors on $\varepsilon_1, \varepsilon_2$ related to each of the noise sources using a definition of two-point correlation function similar to that for shear-shear correlation:

$$C_+(\Delta\theta) = \langle \delta\varepsilon_t(\theta)\delta\varepsilon_t(\theta+\Delta\theta) \rangle + \langle \delta\varepsilon_\times(\theta)\delta\varepsilon_\times(\theta+\Delta\theta) \rangle$$

$$\delta\varepsilon_i = \varepsilon_i - \bar{\varepsilon}_i \quad i = t, \times$$

where $\langle\ \rangle$ denotes averaging over all pairs of object separated by angular distance $\Delta\theta$, and $t, \times$ are the tangential and cross-component of the ellipticity along the line joining the pair of objects.

Results summarized in Figure 6. below:

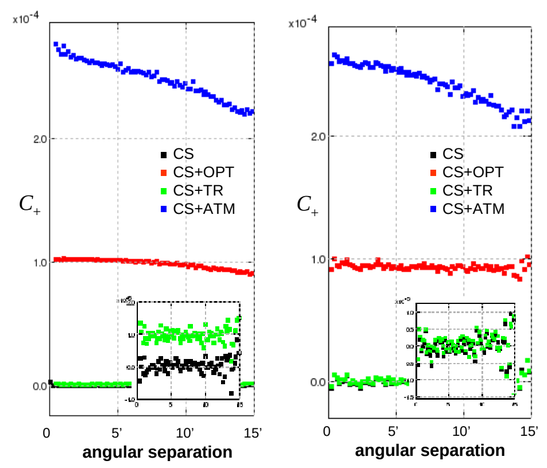

Fig.6 Correlation of errors on $\varepsilon_1, \varepsilon_2$ from different noise sources plotted against angular separation in arc minutes. In both plots we choose objects of FWHM ~1” as a representable example of a typical galaxy. The two plots are plotted for objects of 18 (left) and 20 (right) scaled magnitudes. Note that the green points are close to but higher than the black ones, as shown by the zoomed in view in the lower right corner of each plot.

Figure 6 shows that the dominant sources of correlation noise are the atmospheric and optics aberrations, as expected. These are independent of magnitude, as can be seen from comparison of the two figures.

Conclusion

1. The LSST Monte Carlo code is well suited to enabling quantitative estimation of shape errors due to a wide variety of sources.
2. For single LSST exposures, counting statistics dominates the shape estimation errors for all but the brightest and least extended objects.
3. The correlation noise is dominated by the atmosphere on spatial scales of ~15’ or less.
4. For multiple exposures, we expect the shape errors to be reduced by $1/N^{0.5}$, and the correlation noise to be reduced by $1/N$.
5. This preliminary study suggests that these contributions will not present a serious limitation to cosmic shear measurements with LSST.

[4][5][6] IMSIM documents http://lsstdev.ncsa.uiuc.edu/trac/wiki/LSSTImageSim
[7] Bertin and Arnouts 1996 [8] Nick Kaiser, 2003

Large Synoptic Survey Telescope